

Quasi-Simultaneous Flux Emergence in the Events of October – November 2003

Guiping Zhou · Jingxiu Wang · Yuming Wang ·
Yuzong Zhang

Received: 29 October 2006 / Accepted: 14 August 2007 / Published online: 26 September 2007
© Springer Science+Business Media B.V. 2007

Abstract From late October to the beginning of November 2003, a series of intense solar eruptive events took place on the Sun. More than six active regions (ARs), including three large ARs (NOAA numbers AR 10484, AR 10486, and AR 10488), were involved in the activity. Among the six ARs, four of them bear obviously quasi-simultaneous emergence of magnetic flux. Based on the global H α and SOHO/EIT EUV observations, we found that a very long filament channel went through the six ARs. This implies that there is a magnetic connection among these ARs. The idea of large-scale magnetic connectivity among the ARs is supported by the consistency of the same chirality in the three major ARs and in their associated magnetic clouds. Although the detailed mechanisms for the quasi-simultaneous flux emergence and the large-scale flux system formation need to be extensively investigated, the observations provide new clues in studying the global solar activity.

Keywords Sun: activity · Sun: magnetic fields · Sun: interior

1. Introduction

The extraordinary episodes in October–November 2003 marked some of the most intense solar activity in the 23rd solar cycle, manifesting extremely powerful X-class flares (Donea and Lindsey, 2005; Hurford *et al.*, 2006; Kane, McTiernan, and Hurley, 2005; Schmieder *et al.*, 2006), fast coronal mass ejections (CMEs) (Gopalswamy *et al.*, 2005a, 2005b; Wang *et al.*, 2005), solar energetic particle (SEP) events (Bieber *et al.*, 2005; Jackman *et al.*, 2005; Klassen *et al.*, 2005; Malandraki *et al.*, 2005), interplanetary shocks (Skoug *et al.*, 2004;

G. Zhou (✉) · J. Wang · Y. Zhang
The National Astronomical Observatories, Chinese Academy of Sciences, Beijing 100012, China
e-mail: zhougp@ourstar.bao.ac.cn

Y. Wang
Space Science, University of Science & Technology of China, Hefei, Anhui 230026, China

Y. Zhang
Astronomy Department, Beijing Normal University, Beijing 100875, China

Tokumaru *et al.*, 2005), and large geomagnetic disturbances (Kappenman, 2005; Rosenqvist *et al.*, 2005; Xie *et al.*, 2006). These episodes were abundantly observed by several space-borne and ground-based observatories, and their consequent effects have been analyzed by many investigators (Seppälä *et al.*, 2004; Bhardwaj *et al.*, 2005; Burlaga, Ness, and Stone, 2005; Crider *et al.*, 2005; Farrugia *et al.*, 2005; Gardner *et al.*, 2005; Intriligator, Sun, and Dryer, 2005;Looper, Blake, and Mewaldt, 2005; López-Puertas, Funke, and Gil-López, 2005; Rohen *et al.*, 2005; Shprits *et al.*, 2006; Tsurutani *et al.*, 2005; Watanabe *et al.*, 2006). The powerful solar eruptions (*i.e.*, most of the 80 CMEs, as well as 143 X-ray flares of GOES C-class and above over the period from 18 October to 8 November 2003) originated primarily from three active regions (ARs) with NOAA numbers AR 10484, AR 10486, and AR 10488 (Gopalswamy *et al.*, 2005b). They were well separated in longitude and located on opposite sides of the equator. In the SOHO/EIT EUV observations, dominant coronal dimming or coronal waves were observed to stretch between these three major, well-separated ARs (Chertok and Grechnev, 2005; Grechnev *et al.*, 2005; Zhang *et al.*, 2007), which appeared as a large-scale CME source region. But it is not clear whether this large-scale coronal dimming region was caused by the instability of a single complicated flux system or by a combination of three or four different flux systems. By revisiting the solar events of October–November 2003, in the uninterrupted MDI magnetograms, we found that new emerging flux in the different ARs (*i.e.*, ARs 10488, 10489, 10491, and 10492) appeared almost simultaneously on the photosphere (Wang, 2004). However, there is no observational evidence to indicate that the emerging flux in one active region triggers the emergence in the other regions. We cautiously call the emerging flux in these four ARs within a short time interval a quasi-simultaneous flux emergence, instead of sympathetic flux emergence. The four ARs together with ARs 10484 and 10486 formed a super activity complex. A natural question is whether these ARs were involved in an individual large-scale flux system or whether the quasi-simultaneous emergence of the photospheric magnetic flux in different regions happened coincidentally. Under either condition, the solar corona can go through large-scale reconfigurations, but the mechanisms for understanding CME initiation may be different.

An AR on the solar surface develops from emerging flux regions (EFRs) (*e.g.*, Zirin, 1972; Glackin, 1975). In an EFR the emergence of a bundle of magnetic flux tubes that form at the bottom of, or just below, the convection zone where the dynamo operates (Parker, 1993) rise because of their buoyancy and eventually break through the photosphere, expanding outward (Spadaro *et al.*, 2004). EFRs were first noticed by Waldmeier (1937) and Ellison (1944). They are identified as new bright H α features generally consisting of two small bright plages, which are connected by roughly parallel dark arches in H α observations (Glackin, 1973). The two polarities of an EFR expand and separate as a function of time, which prompted Zirin (1972) to suggest the term EFR. The emerging flux triggering model is established for both solar flares (*e.g.*, Heyvaerts, Priest, and Rust, 1977) and CMEs (Lin *et al.*, 1998; Chen and Shibata, 2000). The distribution and evolution of EFRs are thought to totally determine the appearance of the activity complexes of ARs (Glackin, 1973). If these six ARs were indeed involved in a large-scale flux system, which pre-existed below the photosphere, the global flux emergence would power the very energetic solar events in October–November 2003. In such a case the initiation of CMEs as large-scale solar eruptive events could be understood physically by carefully investigating the related large-scale source magnetic structures.

Zhou, Wang, and Zhang (2006) categorized the sources of halo CMEs from March 1997 to December 2005 into four groups of large-scale magnetic structures: (1) extended bipolar regions (EBRs), (2) trans-equatorial magnetic loops, (3) trans-equatorial filaments and their

associated magnetic structures (*e.g.*, Wang *et al.*, 2006), and (4) long filaments along the boundaries of EBRs. This identification was the first step in building a relationship between CMEs and large-scale source structures from coronal morphologies. The source magnetic structures of the events in October–November 2003 were grouped into the second category, trans-equatorial magnetic loops. The evolution of solar corona is controlled by the photospheric magnetic field. These coronal magnetic fields also originally come from the sub-photosphere as a result of magnetic buoyancy (Parker, 1955). Therefore, photospheric motions can perturb the photospheric footpoints of coronal field lines and drive the coronal evolution (Magara, 2006). In response to the new emerging flux in the different ARs from below the photosphere, the existing coronal field structures, (*e.g.*, the trans-equatorial loops) may be destabilized and cause a variety of large-scale coronal dynamic phenomena (*e.g.*, large-scale dimming and CMEs). In this scenario, the related large-scale source structure in the corona plays an important role in CME initiation. It is interesting to study the relationship between CME initiation and its large-scale source magnetic structures.

The current study attempts to investigate the magnetic connections among the six ARs related to the powerful solar activities in October–November 2003. The basic logic of this paper is to first identify the quasi-simultaneous flux emergence from the MDI 96-min magnetic charts, then to search the magnetic connections among the ARs based on multiwavelength observations, and finally to search for evidence for large-scale magnetic connection. In Section 2 we present a detailed description of the observations. A discussion and conclusions are given in Section 3.

2. Observations and Results

The primary database we used consisted of 96-min-cadence MDI magnetograms, in which the flux emergence on the photosphere can be adequately revealed for a single AR. We rotated all the magnetic data to 11:11 UT on 28 October 2003 to compensate for solar rotation. Full-disk SOHO/EIT EUV and H α images from the Big Bear Solar Observatory (BBSO) were examined to find the connection features. MDI synoptic charts provide a good source to reconstruct 3D magnetic structures in the corona. In addition, Huairou vector magnetograms and the plasma data from ACE were necessary supplements used to calculate the helicity sign of ARs and AR-associated interplanetary magnetic clouds.

2.1. Quasi-Simultaneous Flux Emergence

The commonly accepted idea is that the powerful solar eruptive events in October–November of 2003 are related to three large ARs (10484, 10486, and 10488). The behavior of the other smaller ARs (10489, 10491, and 10492; see the right panel of Figure 1) distributed between the three major ARs have almost a negligible contribution. By revisiting the movie made of the 96-min MDI magnetograms in October–November 2003, we found that the emerging flux in ARs 10489, 10491, and 10492 appeared almost simultaneously with that in AR 10488 (*e.g.*, Wang, 2004). At SOHO/EIT EUV wavelengths, a large-scale EUV dimming was observed between the three major ARs (Chertok and Grechnev, 2005; Grechnev *et al.*, 2005; Wang *et al.*, 2005; Zhang *et al.*, 2007). We suspected that the six ARs perhaps belong to a large-scale complicated flux system.

The six ARs were well separated in longitude and were located on two hemispheres; in each the polarity order followed Hale's law (see the right panel of Figure 1). ARs 10489 and 10491 were located in the domain between ARs 10486 and 10488, and AR 10492 was

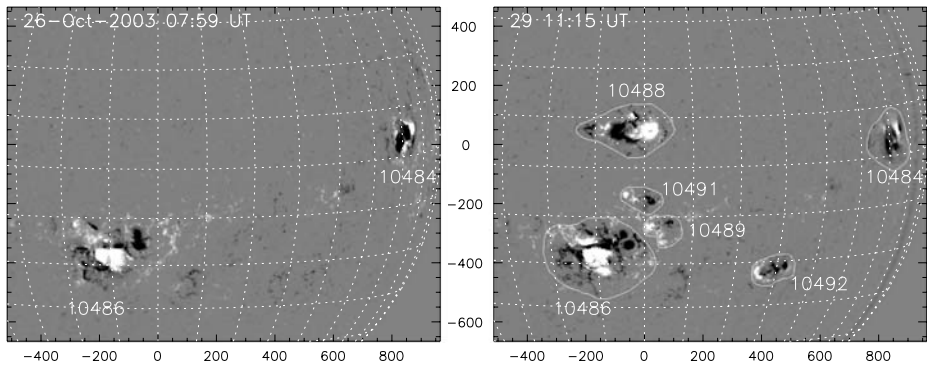


Figure 1 Two MDI images showing the six ARs. ARs 10484 and 10486 have already emerged when they first rotated to the visible solar disk (left panel). The ARs bearing quasi-simultaneous flux emergence (*i.e.*, ARs 10488, 10489, 10491, and 10492) appeared on the photosphere after 07:59 UT on 26 October 2003. The contoured area in the right panel indicates the regions in which we calculate the magnetic flux in the ARs. The time profiles of the AR magnetic flux are shown in Figure 2.

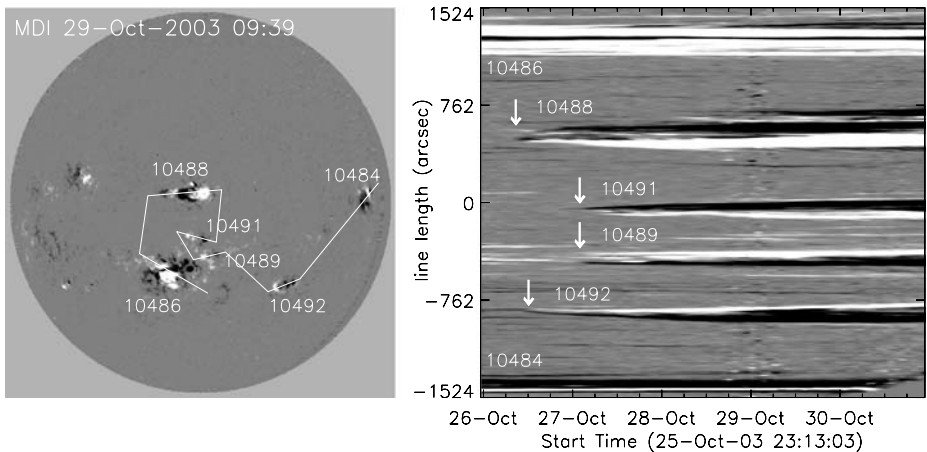


Figure 2 The time evolutions (right panel) of MDI magnetic flux density along a line across the six ARs (left panel). For the line's straight length from right, center, to the left, the positions correspond to -1524 , 0 , and 1524 arcsec, respectively, in the ordinate of the right panel. The MDI flux density evolutions along the line cover the time period from 23:13 UT on 25 October to 22:24 UT on 30 October 2003 with an interval of 96 min.

situated between AR 10484 and AR 10486. The time difference of the new flux emergence in the six ARs can be well seen in the time evolutions of MDI flux density along a line (see the white line in the left panel of Figure 2). We tried to draw a line along the direction of the most intense flux emergence in all ARs, excluding AR 10486, that was too complex for this purpose. The time interval for the right panel of Figure 2 was from 23:13 UT on 25 October to 22:24 UT on 30 October. In MDI observations, ARs 10484 and 10486 had already been on the photosphere when they rotated to the visible solar disk. Magnetic flux in AR 10488 began to emerge at 07:59 UT on 26 October 2003. Following its emergence, ARs 10489, 10491, and 10492 successively appeared on the photosphere (see the right panel of

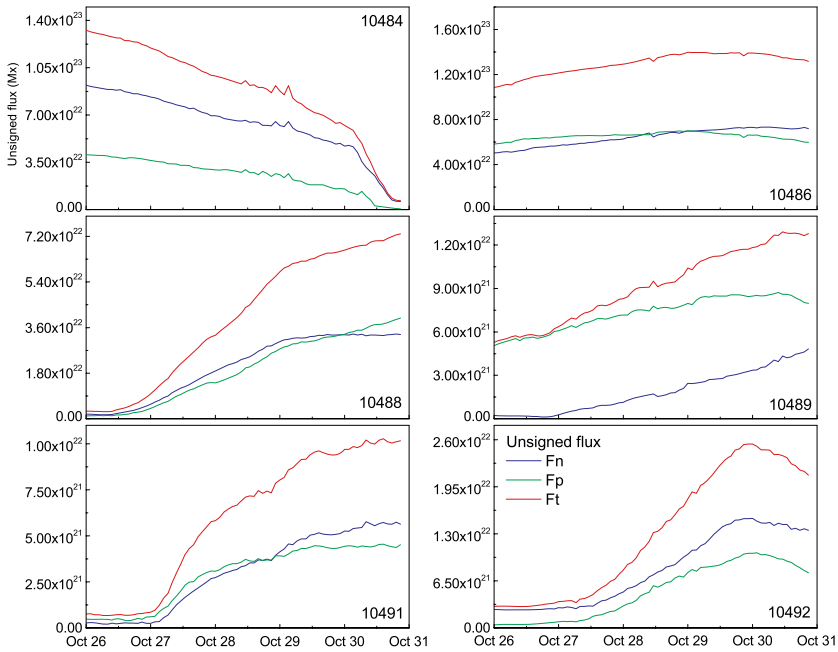


Figure 3 The unsigned emerging flux with time variations in each of the contoured ARs (indicated in Figure 1) shown with positive (F_p , green color), negative (F_n , blue color), and total ($F_t = F_p + F_n$, red color) flux from 23:59 UT on 26 October to 20:48 UT on 30 October.

Figure 2). These four ARs (*i.e.*, 10488, 10492, 10489, and 10491) bore quasi-simultaneous flux emergence.

The emerging flux in the six ARs as a function of time is presented in detail in Figure 3. The region of each AR is denoted by the white contours in the right panel of Figure 1. The projection effect of the calculated line-of-sight flux was simply reduced by dividing magnetic flux by the square of the cosine value of the angle between the magnetic element’s radial and Sun–Earth direction. It has been shown that the flux densities in MDI measurements are on average 0.64 and 0.63 times lower compared to those of the Advanced Stokes Polarimeter (ASP, Berger and Lites, 2003) and Huairou magnetogram (Wang, Ye, and Wang, 2003), respectively. Assuming the ASP data can be adopted as a reference, we further corrected the obtained emerging flux from MDI measurements by dividing it by a factor of 0.64. Since the response of a filter-based magnetograph becomes nonlinear above 1200 G, there is a source of uncertainty in the MDI flux measurements. This result would especially have an impact on the AR with intense magnetic fields (*e.g.*, AR 10486).

In Figure 3, the green, blue, and red curved lines represent positive (F_p), negative (F_n), and total ($F_t = F_p + F_n$) unsigned magnetic flux in each AR. From 23:59 UT on 26 October to 20:48 UT on 30 October, both ARs 10484 and 10486 had nearly matured, and not much new flux emerges. Since a part of AR 10484 continually rotated to the far side of the Sun during this period, the measured flux for the AR gradually decreased. The magnetic fields in AR 10486 were very intense, and fields greater than 1200 G must be strongly influenced by the nonlinear uncertainty in MDI flux measurements. So there should be some deviations for the curves of AR 10486 field evolutions. ARs 10488, 10489, 10491, and 10492 all emerged in the visible hemisphere of the Sun, as evident by at least one polarity (positive or negative)

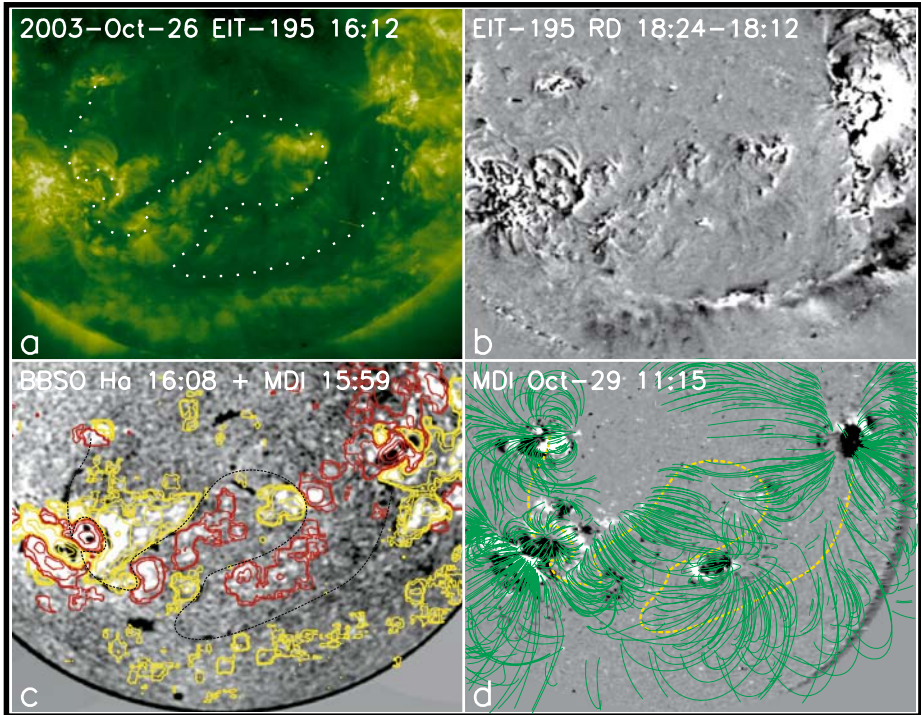


Figure 4 A long filament channel is identified and suggests a connection among the six ARs based on multi-wavelength observations. (a) An EIT 195 Å image at 16:12 UT on 26 October showing the long filament channel as a long narrow dark EUV feature (see the long dotted curve). (b) An EIT running difference (RD) image obtained by subtracting the EUV data at 18:12 from the one at 18:24 UT, which shows coronal dimming along the long filament channel accompanying the associated AR activity. The very long filament channel is situated at a long magnetic neutral line as denoted in panel (c). (c) An H α image at 15:59 on 26 October with contours of nearly simultaneous MDI data. (d) Multiple magnetic arcades overlaying the very long filament channel determined by the method of global potential extrapolation (Wang, Yan, and Wang, 2002). Its background image is an MDI magnetogram at 11:15 UT on 29 October denoting the locations of the six ARs and the long filament channel. The long yellow curve in the figure denote the long filament channel.

flux emerging from a very low level close to zero during this time period for each AR. The four ARs might appear as quasi-simultaneous flux emergence because they emerged on the photosphere with short time intervals (see Figure 3). Because the four ARs are located on opposite hemispheres, it is interesting to investigate their magnetic connection and the physical mechanism based on observations and analysis at other wavelengths.

2.2. A Long Filament Magnetic Channel

By tracking the SOHO/EIT EUV observations from 24 October when AR 10484 fully appeared in the visible solar disk, it was found that a very long EUV dark feature extended from AR 10484, over AR 10486, even to the place where AR 10488 was emerging (the dotted curved line in Figure 4a). After 27 October, when ARs 10488, 10492, 10489, and 10491 all successively emerged on the photosphere (see Figures 2 and 3), the long EUV dark feature indicated some kind of connectivity among the six ARs. In the SOHO/EIT EUV running difference (RD) images, the connectivity among the six ARs along the long

EUV dark feature is revealed by continued channeled coronal dimming, which accompanied the AR activity (*i.e.*, flares, filament eruptions, and coronal surges occurring in ARs 10484 and 10486). As shown in Figure 4b, the RD image obtained by subtracting the EUV data at 18:12 UT from the one at 18:24 UT showed clear coronal dimming along the long EUV dark feature including the region from AR 10486 to AR 10488. Normally, filaments often show themselves as long or short narrow dark features in EUV observations. Whether this long EUV dark feature was a long filament or not should be checked in H α observations.

A filament is thought to be an aggregate of coronal plasma that has lower temperature and higher density than values typical of its surrounding coronal structures. It is often identified in H α observations by its absorption properties. On 26 October, when the long EUV dark feature was almost symmetric to the central longitude, its H α counterpart, appearing as a long filament channel, was obviously present in the H α images from BBSO. But the dark filament materials were not always clearly observed in the whole long filament channel. We cautiously regarded the identified long EUV/H α magnetic feature as a very long filament channel, which indeed was the position where the filament was projected on the photosphere. A filament magnetic channel supports the filament material and is typically oriented along photospheric magnetic neutral lines. The width of a filament magnetic channel is typically of the order of 100 arcsec in EUV images (EIT images, for example) and 50 arcsec in H α images. Thus a long filament channel in the H α images appears weaker than its counterpart in EUV observations. Figure 4c shows an H α image at 15:59 UT on 26 October with contours of nearly simultaneous MDI data. To show the long H α filament channel clearly, we smoothed the H α image over every 4 pixels and displayed it in a limited range (see the long yellow curve in Figure 4c).

A magnetic system where a filament is located often includes the filament, the polarity inversion line (*i.e.*, the projection of the filament place on the photosphere), and multiple magnetic arcades overlaying the filament. As an examination, in Figure 4c, we superposed the contour of a close-time MDI magnetogram on the H α image at 15:59 UT on 26 October. Since most of the long filament was situated near the polar region of the Sun, where the magnetic field was very weak, we smoothed the MDI data over 20 pixels and plotted the contours at levels of 2, 5, 10, 30, 100, 500, and 800 gauss for positive flux density and -800 , -500 , -300 , -100 , -30 , -10 , and -7 gauss for negative flux density. This showed that the long filament channel lay at a long magnetic neutral line on the photosphere. By the method of potential extrapolations (Wang, Yan, and Wang, 2002), the 3D magnetic configurations around the long filament channel were reconstructed based on the MDI synoptic charts in Carrington rotation 2009. The extrapolation result is shown in Figure 4d, where the background image was the MDI magnetogram at 11:15 UT on 29 October used to denote the locations of the six ARs and the long filament channel (see the long yellow curved line). The figure illustrates that there were multiple arcades overlaying the long filament channel. The arcades were aggregately connected. With the identification of the long filament channel, the question of whether or not the ARs that are coupled by the long filament channel belong to a single complex magnetic flux system needs further investigation.

2.3. Further Evidence for the Large-Scale Magnetic Connectivity

As suggested by Wang (1996) and Wang, Zhou, and Zhang (2004), an individual flux system tends to have a predominant chirality in most cases; therefore can be simulated by a constant- α force-free field. To identify the dominant sign of the chirality of the ARs, we assume that the solar magnetic fields are force free, that is, $\nabla \times \mathbf{B} = \alpha \cdot \mathbf{B}$, where α is the force-free coefficient that can be observationally estimated, and extrapolate force-free fields that can

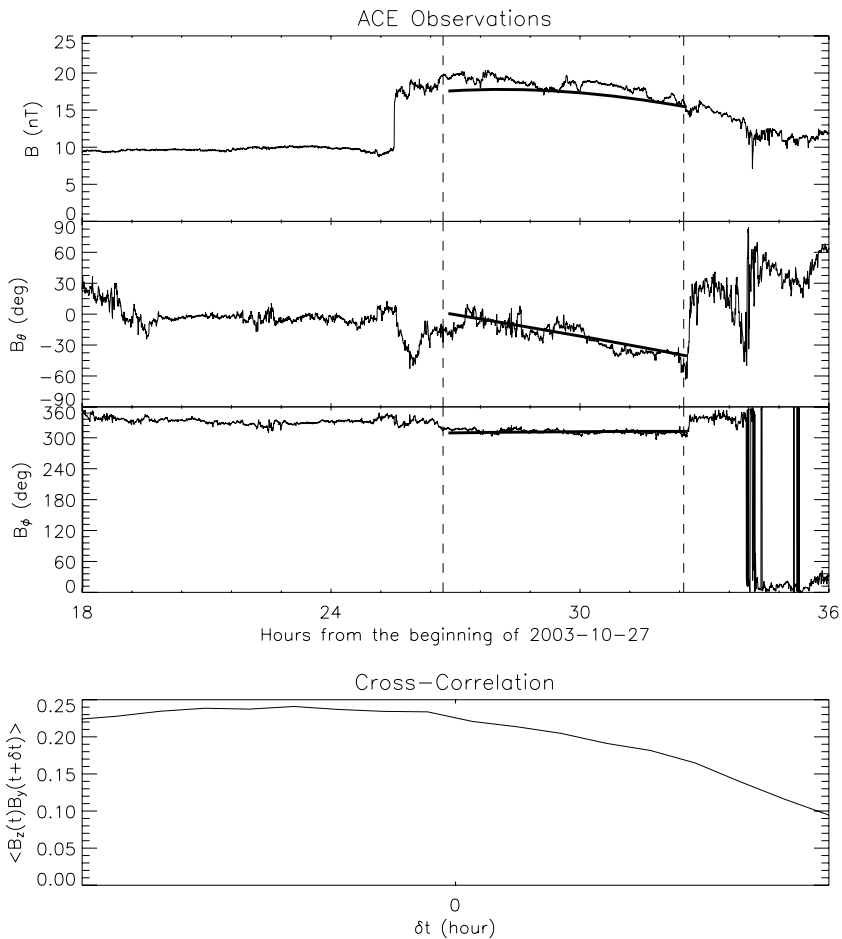


Figure 6 Top panel: The fitting results of the AR 10484-associated magnetic cloud determined by using a force-free cylindrical flux rope model. The estimated chirality of the cloud is left-handed, and the orientation of the cloud is at approximately 327° longitude and -6° latitude in GSE coordinates. Bottom panel: Cross-correlation as a function of δt for the AR 10484-associated magnetic cloud. The sign of the magnetic helicity is the same as the sign of the curve’s slope at $\delta t = 0$, which, in this case, indicates a left-handed chirality.

field of view. The first method was to fit the observed data with a force-free flux rope model (e.g., Lepping, Jones, and Burlaga, 1990; Wang, Ye, and Wang, 2003), in which the parameters of the magnetic field configuration of the magnetic cloud could be obtained. In the second method, called the cross-correlation approach (see Matthaeus and Goldstein, 1982; Ruzmaikin, Martin, and Hu, 2003), information about the magnetic helicity is stored in the cross-correlation of different components of the magnetic field, $C(\delta t) = \langle B_z(t)B_y(t + \delta t) \rangle$, and the sign of helicity is the same as the slope of $C(\delta t)$ at $\delta t = 0$. As had been done in Wang *et al.* (2005), the helicity sign of the AR 10486-associated magnetic cloud was negative, indicating a left-handed chirality.

On 28 October, the other magnetic cloud was identified related to AR 10484. By using the method of a force-free cylindrical flux rope model (Xiao *et al.*, 2004), the boundary and

orientation of the magnetic cloud structure was determined. Here we used the same two methods to analyze the chirality of this magnetic cloud. The associated CME first appeared at 17:40 UT on 26 October in the LASCO C2 field of view. The top panel of Figure 6 shows the fitted results of the magnetic cloud based on the first method. The orientation (*i.e.*, the direction of the axial magnetic field) of the cloud was estimated as approximately 327° longitude and -6° latitude. The indicated chirality of this magnetic cloud is left-handed. The bottom panel of Figure 6 shows the profile of C , which suggests that the helicity of the cloud was negative (*i.e.*, left-handed chirality). Thus the three ARs in the October–November events in 2003 and their associated magnetic clouds all had the same chirality. The results are consistent with the thought that these ARs probably belong to one large-scale magnetic flux system.

3. Discussion and Conclusions

In this work, we had investigated the quasi-simultaneous flux emergence in the events of October–November 2003 with a focus on the magnetic connections among the six ARs. As a result, a large-scale intercoupled magnetic flux system was proposed to build a magnetic connection among the six associated ARs. The physical process of the instability in the large-scale flux system was believed to be responsible for the generation of the solar flares and CMEs during that period. Principal analysis and results in our study are summarized as follows:

1. On 26 October 2003, the magnetic flux in AR 10488 first emerged at 09:35 UT as shown by MDI magnetograms. Following its flux emergence, flux in ARs 10492, 10491, and 10489 successively emerged at 12:47 UT, 19:11 UT, and 20:47 UT (see Figure 3). The flux emergence in these four ARs appeared to be quasi-simultaneous.
2. Based on the full-disk observations of SOHO/MDI, SOHO/EIT EUV, and $H\alpha$ from BBSO, it was found that a large-scale magnetic connection, represented as a long filament channel, coupled the six ARs.
3. The idea that the six ARs probably originated from one large-scale active nest was also supported by evidence of the same chirality in ARs 10484, 10486 and 10488 as well as in their associated magnetic clouds. However, it should be mentioned that this result was obtained with the approximation of constant- α force-free magnetic fields, which may oversimplify the actual solar magnetic fields.

The results indicate that a few ARs or AR-scale activity may be in fact part of a certain type of large-scale magnetic flux system, which would be an intrinsic component of solar magnetism. The instability of the large-scale flux system, and/or its interaction with other magnetic systems, may be the origin of the prolific CME initiation. The physical mechanism of the quasi-simultaneous flux emergence and how these ARs are connected by a large-scale magnetic structure are topics of future studies. To answer these questions, high-resolution Dopplegrams and full-Sun vector magnetograms are required. Moreover, it is important to analyze the dynamics of plasma in the solar interior and three-dimensional maps of plasma flows through the whole convection zone.

The quasi-simultaneous flux emergence during October–November 2003 provides an important clue to understanding the extremely intense activity in a solar cycle. Although flux emergence in several ARs is observed successively with short intervals, we are not sure whether such flux emergence is sympathetic because we cannot identify the propagating agent that causes the sympathy of flux emergence in widely separated locations on the Sun. We also seem unable to exclude the possibility that we indeed observed a sympathetic flux emergence in the intense activity period.

Acknowledgements We are grateful to all members of the SOHO EIT, LASCO, and MDI teams, ACE and *Wind* teams, and the Huairou staff for providing the wonderful data. SOHO is a project of international cooperation between ESA and NASA. We also thank the anonymous referees for their constructive comments and suggestions. The work is supported by the National Natural Science Foundation of China (10603008, 40636031, 40504021, 40674081, 10573025, and 40525014), CAS Project KJXC2-YW-T04, and the National Key Basic Research Science Foundation (2006CB806303).

References

- Berger, T.E., Lites, B.W.: 2003, *Solar Phys.* **213**, 213.
- Bhardwaj, A., et al.: 2005, *Geophys. Res. Lett.* **32**, L03. S08
- Bieber, J.W., et al.: 2005, *Geophys. Res. Lett.* **32**, L03S02.
- Burlaga, L.F., Ness, N.F., Stone, E.C.: 2005, *Geophys. Res. Lett.* **32**, L03S05.
- Chen, P.F., Shibata, K.: 2000, *Astrophys. J.* **545**, 524.
- Chertok, I.M., Grechnev, V.V.: 2005, *Astron. Rep.* **49**, 2.
- Crider, D.H., et al.: 2005, *J. Geophys. Res.* **110**, A09S21.
- Donea, A.-C., Lindsey, C.: 2005, *Astrophys. J.* **630**, 1168.
- Ellison, M.A.: 1944, *Mon. Not. R. Astron. Soc.* **104**, 22.
- Farrugia, C.J., et al.: 2005, *J. Geophys. Res.* **110**, A09S13.
- Gardner, J.L., et al.: 2005, *J. Geophys. Res.* **110**, A09S34.
- Glackin, D.L.: 1973, *Publ. Astron. Soc. Pac.* **85**, 241.
- Glackin, D.L.: 1975, *Solar Phys.* **43**, 317.
- Gopalswamy, N., et al.: 2005a, *J. Geophys. Res.* **110**, A09S15.
- Gopalswamy, N., et al.: 2005b, *J. Geophys. Res.* **110**, A09S00.
- Grechnev, V.V., et al.: 2005, *J. Geophys. Res.* **110**, A09S07.
- Hagyard, M.J., Pevtsov, A.A.: 1999, *Solar Phys.* **189**, 25.
- Heyvaerts, J., Priest, E.R., Rust, D.M.: 1977, *Astrophys. J.* **216**, 123.
- Hurford, G.J., et al.: 2006, *Astrophys. J.* **644**, L93.
- Intriligator, D.S., Sun, W., Dryer, M.: 2005, *J. Geophys. Res.* **110**, A09S10.
- Jackman, C.H., et al.: 2005, *J. Geophys. Res.* **110**, A09S27.
- Kane, S.R., McTiernan, J.M., Hurley, K.: 2005, *Astron. Astrophys.* **433**, 1133.
- Kappenman, J.G.: 2005, *Space Weather* **3**, S08C01.
- Klassen, A., et al.: 2005, *J. Geophys. Res.* **110**, A09S04.
- Lepping, R.P., Jones, J.A., Burlaga, L.F.: 1990, *J. Geophys. Res.* **95**, 11957.
- Lin, J., et al.: 1998, *Astrophys. J.* **504**, 1006.
- Liu, J.H., Zhang, H.Q.: 2006, *Solar Phys.* **234**, 21.
- Looper, M.D., Blake, J.B., Mewaldt, R.A.: 2005, *Geophys. Res. Lett.* **33**, L03S06.
- López-Puertas, M., Funke, B., Gil-López, S.: 2005, *J. Geophys. Res.* **110**, A09S43.
- Magara, T.: 2006, *Astrophys. J.* **653**, 1499.
- Malandraki, O.E., et al.: 2005, *J. Geophys. Res.* **110**, A09S06.
- Matthaeus, W.H., Goldstein, M.L.: 1982, *J. Geophys. Res.* **87**, 6011.
- Parker, E.N.: 1955, *Astrophys. J.* **121**, 491.
- Parker, E.N.: 1993, *Astrophys. J.* **408**, 707.
- Pevtsov, A.A., Canfield, R.C., Metcalf, T.R.: 1994, *Astrophys. J.* **425**, L117.
- Rohen, G., et al.: 2005, *J. Geophys. Res.* **110**, A09S39.
- Rosenqvist, L., et al.: 2005, *J. Geophys. Res.* **110**, A09S23.
- Ruzmaikin, A., Martin, S., Hu, Q.: 2003, *J. Geophys. Res.* **108**(A2), 1096.
- Schmieder, B., et al.: 2006, *Adv. Space Res.* **37**, 1313.
- Seppälä, A., et al.: 2004, *Geophys. Res. Lett.* **31**, L19107.
- Shprits, Y.Y., et al.: 2006, *Geophys. Res. Lett.* **33**, L05104.
- Skoug, R.M., et al.: 2004, *J. Geophys. Res.* **109**, A09102.
- Spadaro, D., et al.: 2004, *Astron. Astrophys.* **425**, 309.
- Tokumaru, M., et al.: 2005, *J. Geophys. Res.* **110**, A01109.
- Tsurutani, B.T., et al.: 2005, *Geophys. Res. Lett.* **32**, L03S09.
- Waldmeier, M.: 1937, *Z. Astrophys.* **14**, 91.
- Wang, J.X.: 1996, *Solar Phys.* **163**, 319.
- Wang, J.X.: 2004, *Proc. IAU Symp.* **223**, 3.
- Wang, J.X., Zhou, G.P., Zhang, J.: 2004, *Astrophys. J.* **615**, 1021.
- Wang, J.X., et al.: 2006, *Chin. J. Astron. Astrophys.* **6**, 247.

- Wang, T., Yan, Y., Wang, J.: 2002, *Astrophys. J.* **572**, 580.
- Wang, Y.M., Ye, P.Z., Wang, S.: 2003, *J. Geophys. Res.* **108**(A10), 1370.
- Wang, Y.M., et al.: 2005, *Solar Phys.* **226**, 337.
- Watanabe, K., et al.: 2006, *Astrophys. J.* **636**, 1135.
- Xiao, C.J., et al.: 2004, *J. Geophys. Res.* **109**, A11218.
- Xie, Y.Q., et al.: 2006, *Solar Phys.* **234**, 363.
- Zhang, Y.Z., et al.: 2007, *Solar Phys.* **241**, 329.
- Zhou, G.P., Wang, J.X., Zhang, J.: 2006, *Astron. Astrophys.* **445**, 1133.
- Zirin, H.: 1972, *Solar Phys.* **22**, 34.